Operator entanglement in SU(2)-symmetric dissipative quantum many-body dynamics

Lin Zhang[1⋆]

1 ICFO-Institut de Ciencies Fotoniques, The Barcelona Institute of Science and Technology, Av. Carl Friedrich Gauss 3, 08860 Castelldefels (Barcelona), Spain

⋆ lin.zhang@icfo.eu

Abstract

The presence of symmetries can lead to nontrivial dynamics of operator entanglement in open quantum many-body systems, which characterizes the cost of an matrix product density operator (MPDO) representation of the density matrix in the tensor-network methods and provides a measure for the corresponding classical simulability. One example is the U(1)-symmetric open quantum systems with dephasing, in which the operator entanglement increases logarithmically at late times instead of being suppressed by the dephasing. Here we numerically study the far-from-equilibrium dynamics of operator entanglement in a dissipative quantum many-body system with the more complicated SU(2) symmetry and dissipations beyond dephasing. We show that after the initial rise and fall, the operator entanglement also increases again in a logarithmic manner at late times in the SU(2)-symmetric case. We find that this behavior can be fully understood from the corresponding U(1) subsymmetry by considering the symmetry-resolved operator entanglement. But unlike the U(1)-symmetric case with dephasing, both the classical Shannon entropy associated with the probabilities for the half system being in different symmetry sectors and the corresponding symmetry-resolved operator entanglement have nontrivial contributions to the late time logarithmic growth of operator entanglement. Our results show evidence that the logarithmic growth of operator entanglement at long times is a generic behavior of dissipative quantum many-body dynamics with U(1) as the symmetry or subsymmetry and for more broad dissipations beyond dephasing. We show that the latter is valid even for open quantum systems with only U(1) symmetry by breaking the SU(2) symmetry of our quantum dynamics to U(1).

Contents

1 Introduction

Recent years have witnessed remarkable experimental advances in atomic, molecular, and optical physics, which have enabled us to engineer quantum many-body systems in controllable and clean environments at the level of individual atoms, molecules, and ions [1–5]. These achievements provide us insights into the studies of strongly correlated quantum systems [6–9]. Among them, extensive attention has been focused on understanding quantum many-body dynamics far away from equilibrium [10, 11], an outstanding challenge in the modern physical sciences, and many new states of matter have been uncovered, such as the many-body localization [12, 13], time crystals [14, 15], and quantum many-body scars [16, 17]. However, it is usually hard to characterize these nonequilibrium systems.

One important tool to describe the quantum many-body dynamics is the so-called entanglement entropy. On the one hand, its growth as a function of time can show fundamentally distinct behavior in different nonequilibrium systems. For instance, the growth of entanglement entropy is logarithmic in the many-body localized models [18], while it increases linearly for a generic chaotic system. This provides a defining feature for many nonequilibrium states of matter. On the other hand, the growth of entanglement entropy also provides insights into the classical simulations of quantum many-body dynamics using tensor networks [19–21]. In one dimension (1D), the quantum states can be faithfully represented by matrix-product states (MPSs) in terms of local rank-three tensors with bond dimension χ [22, 23], for which the entanglement entropy is bounded by $\log_2 \chi$. Thus the linear increase of entanglement entropy will lead to an exponential growth of bond dimension, which is considered to be hard to simulate [24]. Only the quantum dynamics within a low-entanglement manifold of the Hilbert space can be efficiently simulated on classical computers. Thanks to the above reasons, studying the growth of entanglement entropy has become one of the central tasks in investigating quantum many-body dynamics and has attracted broad interest [25–28].

The growth of entanglement entropy also helps the understanding of open quantum many-body systems, which are ubiquitous in practical experiments due to the inevitable couplings to environments. Like the MPS representation for pure states, the density matrix of 1D open quantum many-body systems can be described by the matrix product density operators (MPDOs) [29–31]. The bipartition of MPDO through Schmidt decomposition further defines the entanglement entropy in operator space, which is known as the operator entanglement and characterizes the cost of an MPDO representation, i.e., how many Schmidt values are needed at least for faithfully representing an operator [32–37], hence providing a measure for the classical simulability of open quantum many-body systems via the MPDO tensor-network method.

In open quantum systems, after the initial linear growth reminiscent of unitary quantum dynamics, the operator entanglement is expected to be suppressed by the dissipations. However, it was recently reported that the operator entanglement in U(1)-symmetric open quan-

tum many-body systems with dephasing increases logarithmically at long times [38], which is attributed to the growth of classical Shannon entropy associated with the probabilities for the half system being in different U(1) sectors. This highlights the role of symmetries on the operator entanglement dynamics in open quantum many-body systems, which, however, still remains largely unexplored. One important symmetry is the non-Abelian SU(2) symmetry, which is believed to be crucial in many nonequilibrium phenomena like quantum many-body scars [39] and anomalous finite-temperature transport [40]. As the non-Abelian symmetry in general increases the entanglement entropy [41–43], it would be interesting to study how the long-time behavior of operator entanglement is impacted in the presence of SU(2) symmetry. Particularly, as the SU(2)-symmetric open quantum many-body system contains U(1) as the subsymmetry and dissipations beyond dephasing, it would be interesting to know whether the logarithmic growth of operator entanglement can go beyond open quantum systems with U(1) symmetry and dephasing.

In this work, we numerically study the far-from-equilibrium dynamics of operator entanglement in a dissipative quantum many-body system with SU(2) symmetry. We show that after the initial rise and fall, the operator entanglement also increases again in a logarithmic manner at long times in the SU(2)-symmetric case. We find that this behavior can be fully understood from the corresponding U(1) subsymmetry by considering the symmetry-resolved operator entanglement [44–46]. But unlike the U(1)-symmetric case, both the classical Shannon entropy and the symmetry-resolved operator entanglement now have nontrivial contributions to the late time logarithmic growth of operator entanglement. Our results show evidence that the logarithmic growth of operator entanglement at long times is a generic behavior of dissipative quantum many-body dynamics with U(1) as the symmetry or subsymmetry and for more broad dissipations beyond dephasing. We show the latter is even valid for open quantum systems with only U(1) symmetry by breaking the SU(2) symmetry of our quantum dynamics to U(1).

2 Model

We consider the open quantum many-body dynamics on an infinite spin-1/2 chain governed by the Lindblad master equation ($\hbar \equiv 1$)

$$\frac{\mathrm{d}}{\mathrm{d}t}\rho = -\mathrm{i}[H,\rho] + \gamma \sum_i \left(L_i \rho L_i^\dagger - \{L_i^\dagger L_i, \rho\}/2 \right) \equiv \mathcal{L}[\rho], \tag{1}$$

where the Hamiltonian $H = J\sum_i P_{i,i+1}$ with the exchange operator $P_{i,i+1} = 2\mathbf{S}_i \cdot \mathbf{S}_{i+1} + 1/2$ is the 1D Heisenberg model with SU(2) symmetry. Here $\mathbf{S}_i$ denotes the spin-1/2 operator on site i, and J is the nearest-neighbor spin coupling strength. We couple the system to an environment through the Lindblad operator $L_i = P_{i,i+1}$ with strength γ, which describes the dissipation proportional to the dipole interaction between neighbor sites; see Fig. 1(a) for the sketch. Similar model has been considered in Refs. [47,48] to study the stability or absence of superdiffusion in a spin chain with fluctuating exchange couplings that break the integrability. Since L_i commutes with the total spin operator, the above Lindblad master equation preserves the SU(2) symmetry. To study the quantum dynamics with SU(2) symmetry, we consider the initial state $\rho_0 = |\psi_0\rangle\langle\psi_0|$ with $|\psi_0\rangle = \bigotimes_i (|\uparrow\rangle_{2i-1}|\downarrow\rangle_{2i} - |\downarrow\rangle_{2i-1}|\uparrow\rangle_{2i})/\sqrt{2}$, which is the product state of singlet pairs. This state has total spin 0 and is SU(2)-symmetric.

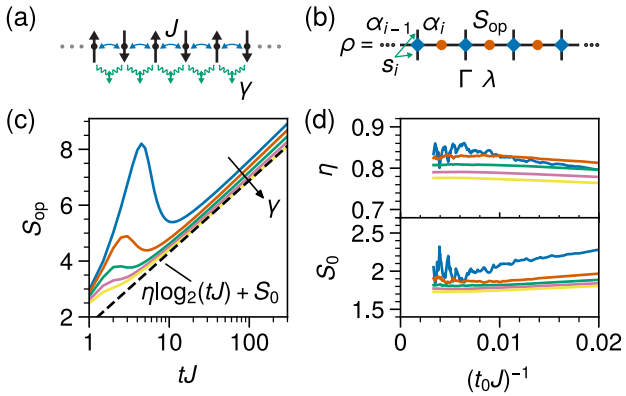

Figure 1: Operator entanglement dynamics in the SU(2)-symmetric dissipative quantum many-body system. (a) Sketch of the model. We consider a quantum spin chain with coherent nearest-neighbor coupling J (blue arrows) and local dissipation proportional to the dipole interaction between neighbor sites with strength γ (green arrows). (b) MPDO decomposition of the density matrix ρ in terms of local tensors Γ (blue squares) and λ (orange circles). Here α_{i-1} and α_i are the bond indices, while s_i denotes the combined physical index of the bra and ket legs at site i. The operator entanglement S_{op} at certain bond can be calculated from the Schmidt vectors λ. (c) Time evolution of S_{op} for the product initial state of singlet pairs with different dissipation strength $\gamma = 0.05J$, $0.10J$, $0.15J$, $0.20J$, and $0.25J$. The black dashed line indicates the logarithmic growth of operator entanglement at long times (log-scale time axis), i.e., $S_{\mathrm{op}}(t \to \infty) = \eta \log_2(tJ) + S_0$. (d) Numerical prefactor η and offset S_0 obtained from the local tangent of operator entanglement at time t_0J. The results are converged for time step $\delta tJ = 0.5$ and maximum bond dimension $\chi = 50000$.

3 MPDO decomposition of density matrix

To solve the Lindblad master equation, we describe the density matrix with MPDO. The matrix product decomposition of density matrix is a mixed-state version of the MPS, where the density matrix ρ of a spin-1/2 chain with local Hilbert space dimension $d = 2$ is treated as a vector $|\rho\rangle_\sharp$ in the tensor product space of the $d \times d$ complex matrices [29]. Here we use the subscript $\sharp$ (sharp) to denote operators (superoperators) when represented as the superkets $|\cdot\rangle_\sharp$ (mappings between superkets), with $\langle s|s'\rangle_\sharp \equiv \mathrm{Tr}(s^\dagger s')/d$. Given a set of orthonormal basis $\{|s_i\rangle_\sharp\}$ for each site i, the density matrix $|\rho\rangle_\sharp$ can be decomposed as

$$|\rho\rangle_\sharp = \sum_{\{s_i\}} \sum_{\{\alpha_i\}} \prod_i \Gamma^{[i]s_i}_{\alpha_{i-1}\alpha_i} \lambda^{[i]}_{\alpha_i} \bigotimes_i |s_i\rangle_\sharp \tag{2}$$

through a succession of Schmidt decompositions [29], where $\Gamma^{[i]}$ is a rank-three tensor on site i with one combined physical index s_i and two bond indices α_{i-1}, α_i, while $\lambda^{[i]}$ is the Schmidt vector on bond i; see Fig. 1(b). Since both the initial state and Liouvillian operator are invariant under the translation by two sites, we have $\Gamma^{[i+2]} = \Gamma^{[i]}$ and $\lambda^{[i+2]} = \lambda^{[i]}$. Therefore, the numerical simulation can be performed within a unit cell of two sites for the infinite lattice, for which only two Γ and λ tensors are needed to capture the density matrix.

For the Liouvillian superoperator (1) that can be decomposed into terms involving at most two contiguous sites, the time evolution can be simulated using the infinite time-evolving block decimation (iTEBD) algorithm with a fourth-order Trotter decomposition of the matrix exponential of the Liouvillian $\exp(\mathcal{L}_\sharp \delta t)$ for a time step δt [21]. We note that since the open quantum many-body dynamics governed by the Lindblad master equation is nonunitary, the

canonical form of the infinite MPDO is in general not preserved in the original iTEBD algorithm [49]. As a consequence, the truncation errors accumulate fast and ruin the simulation at long times. To overcome this issue, we employ the improved algorithm for nonunitary evolutions proposed in Ref. [50], in which the tensors updated in each time step are reorthonormalized into the canonical form. To avoid the exponential growth of bond dimension, we also truncate the tensors $\{\Gamma^{[i]}\}$ and $\{\lambda^{[i]}\}$ at a maximum bond dimension χ. The results shown in this work are all numerically converged.

4 Operator entanglement

We focus on the time evolution of operator entanglement in our SU(2)-symmetric dissipative quantum many-body dynamics. The operator entanglement is a basis-independent measure for quantum operators. Given the MPDO decomposition (2), the operator entanglement at certain bond is defined as [32–37]

$$S_{\mathrm{op}} \equiv -\sum_{\alpha} \lambda_{\alpha}^2 \log_2 \lambda_{\alpha}^2, \tag{3}$$

where the Schmidt values are assumed to be normalized, i.e., $\sum_\alpha \lambda_\alpha^2 = 1$. We note that the operator entanglement does not characterize the quantum entanglement between different parts of the system, which is instead captured by the entanglement measures like entanglement negativities when ρ is a mixed state [51,52]. The operator entanglement mainly reflects the cost of encoding an operator in the MPDO representation and also provides insights into nonequilibrium quantum many-body physics like the quantum chaos and information scrambling [53–55].

For our SU(2)-symmetric quantum dynamics, the total spin $\mathbf{S}_{\mathrm{tot}} = \sum_i \mathbf{S}_i$ is conserved. Therefore, we have $\mathbf{S}_{\mathrm{tot}}^2 \rho = S_{\mathrm{tot}}(S_{\mathrm{tot}}+1)\rho$ during the time evolution, where S_{tot} is zero for our initial state ρ_0 as a product state of singlet pairs. Consider a bipartitioning of the system, $\rho = \sum_\alpha \lambda_\alpha \varrho_\alpha^{[\mathrm{L}]} \otimes \varrho_\alpha^{[\mathrm{R}]}$, with $\langle \varrho_\alpha^{[\mathrm{L/R}]} | \varrho_{\alpha'}^{[\mathrm{L/R}]} \rangle_\sharp = \delta_{\alpha\alpha'}$ for the left (L) and right (R) part. We also have $\mathbf{S}_{\mathrm{L/R}}^2 \varrho_\alpha^{[\mathrm{L/R}]} = S_{\mathrm{L/R}}(S_{\mathrm{L/R}}+1)\varrho_\alpha^{[\mathrm{L/R}]}$ with $S_{\mathrm{L}} = S_{\mathrm{R}} \equiv S$, where $\mathbf{S}_{\mathrm{L/R}}$ is the total spin operator in the left/right part of the system. For this, we can relabel the bond index α as $\alpha \to (S, i_S)$, where i_S distinguishes the Schmidt values (i.e., different half-system density matrices) corresponding to the same half-system total spin S. We note that in our notation the degenerate degrees of freedom of each spin sector S is not counted into i_S. For each bond label (S, i_S), there are actually $(2S+1)$ Schmidt coefficients with the same value $\lambda_{(S,i_S)}$ in our numerical simulation with SU(2) symmetry. Hence the operator entanglement is given by $S_{\mathrm{op}} = -\sum_S \sum_{i_S} (2S+1)\lambda_{(S,i_S)}^2 \log_2 \lambda_{(S,i_S)}^2$ in this notation with the normalization condition $\sum_S \sum_{i_S} (2S+1)\lambda_{(S,i_S)}^2 = 1$. We also remark that the quantum number S can also be defined by multiplying the symmetry operator from the right of density matrix, which does not change the results.

It is useful to also introduce the symmetry-resolved operator entanglement, which has attracted extensive attention recently [56–61]. Specifically, following in Ref. [38], for a generic global symmetry Q, the operator entanglement for the MPDO decomposition (2) at certain bond can be split into different symmetry sectors, similarly to that of the state entanglement [44–46]. The symmetry-resolved operator entanglement in a specific symmetry sector q is defined through the renormalized Schmidt coefficients $\hat{\lambda}_{q,i_q} = \lambda_{q,i_q}/\sqrt{p_q}$ belonging to that sector via $S_{\mathrm{op},q} \equiv -\sum_{i_q} \hat{\lambda}_{q,i_q}^2 \log_2 \hat{\lambda}_{q,i_q}^2$, where i_q labels different Schmidt coefficients in the symmetry sector q and $p_q = \sum_{i_q} \lambda_{q,i_q}^2$ is the probability of having symmetry charge q in the half system such that $\sum_{i_q} \hat{\lambda}_{q,i_q}^2 = 1$. In our SU(2)-symmetric case, different symmetry sectors

are labeled by the half-system total spin S, and the probability of having total spin S in the half system is $p_S = (2S+1)\sum_{i_S} \lambda^2_{(S,i_S)}$ [note that in our notation for the SU(2) symmetry, each bond label (S, i_S) actually corespondents to $(2S+1)$ Schmidt coefficients with the same value λ_{S,i_S}]. Then the symmetry-resolved operator entanglement in the spin sector S is given by $S_{\mathrm{op},S} = -(2S+1)\sum_{i_S} \hat{\lambda}^2_{(S,i_S)} \log_2 \hat{\lambda}^2_{(S,i_S)}$ with $\hat{\lambda}_{(S,i_S)} \equiv \lambda_{(S,i_S)}/\sqrt{p_S}$. With this, the full operator entanglement can be recast as

$$S_{\mathrm{op}} = \sum_S p_S S_{\mathrm{op},S} - \sum_S p_S \log_2 p_S, \tag{4}$$

where the first term describes the averaged contribution from the symmetry-resolved operator entanglement in different spin sectors, while the second term is the classical Shannon entropy of the probability distribution.

Since our model has the U(1) subsymmetry, e.g., the conservation of total magnetization along the z direction, we can also label the Schmidt coefficients via the half-system magnetization and define the corresponding symmetry-resolved operator entanglement; see Refs. [38, 59, 61]. For our SU(2)-symmetric case, since each spin sector with $S \geq |S_z|$ contributes one state to the magnetization sector S_z, we can express the probability of having magnetization S_z in the half system as $p_{S_z} = \sum_{S\geq|S_z|}\sum_{i_S} \lambda^2_{(S,i_S)}$, and the symmetry-resolved operator entanglement in this magnetization sector is given by $S_{\mathrm{op},S_z} = -\sum_{S\geq|S_z|}\sum_{i_S} \tilde{\lambda}^2_{(S,i_S)} \log_2 \tilde{\lambda}^2_{(S,i_S)}$ with $\tilde{\lambda}_{(S,i_S)} \equiv \lambda_{(S,i_S)}/\sqrt{p_{S_z}}$. The relation to the full operator entanglement S_{op} is similar to Eq. (4).

5 Results

5.1 Logarithmic growth of operator entanglement

We now present the numerical results for our open quantum many-body system (1). In Fig. 1(c), we show the time evolution of operator entanglement S_{op} for the product initial state of singlet pairs. Initially, the operator entanglement grows linearly in time, as the quantum dynamics at such short times is dominated by the Hamiltonian part of Eq. (1) and can be approximated to be unitary. However, when $t \gtrsim \gamma^{-1}/4$ in our numerical simulation, the coupling to the environment becomes relevant, and the operator entanglement starts to decrease.

Typically, if there is no conservation law in the dissipative quantum many-body dynamics, the density matrix is expected to relax to the infinite-temperature state (i.e., the identity matrix), and the operator entanglement converges toward the corresponding value of that stationary state at late times. However, the introduction of symmetries can enrich the behavior of operator entanglement. Particularly, it was recently reported that after the initial rise and fall, the operator entanglement in U(1)-symmetric open quantum many-body systems with dephasing increases again in a logarithmic manner at late times, i.e., $S_{\mathrm{op}}(t\to\infty) = \eta \log_2(tJ) + S_0$ [38].

Here we also observe the same behavior of operator entanglement in our dissipative quantum many-body dynamics with SU(2) symmetry; see Fig. 1(c). Especially, we show the prefactor η and offset S_0 as a function of time t_0 in Fig. 1(d), which is obtained as the local tangent of operator entanglement. Due to the limited maximum bond dimension, the data for small γ is not good enough as those for the strongly dissipative cases. However, all of them show the tendency to converge to a finite value as $t_0 \to \infty$, thus identifying the logarithmic growth behavior of operator entanglement at late times. We note that unlike the U(1)-symmetric case with dephasing [38], from the numerical tendency exhibited in Fig. 1(d) both the prefactor η and offset S_0 seem to be nonuniversal and depend on the value of the dissipation strength. However, it should be mentioned that whether η converges universally to a fixed value like

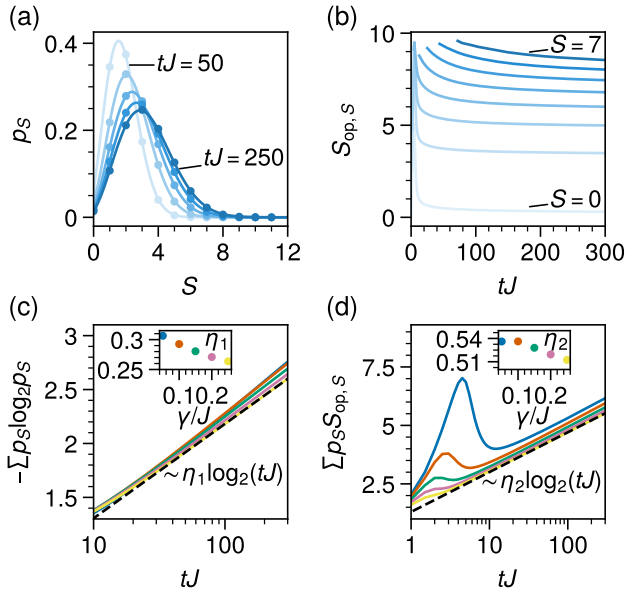

Figure 2: Symmetry-resolved operator entanglement in spin sectors. (a) Probabilities p_S of the infinite chain with total spin S in the half system at increasingly late times ($50 \leq tJ \leq 250$ from light to dark) for $\gamma = 0.05J$. The lines are fits with the trial function shown in the main text. (b) The corresponding symmetry-resolved operator entanglement $S_{\mathrm{op},S}$ as a function of time. Only the data with probabilities $p_S > 10^{-4}$ are presented. (c) (d) The classical Shannon entropy $-\sum p_S \log_2 p_S$ and the averaged symmetry-resolved operator entanglement $\sum p_S S_{\mathrm{op},S}$ as a function of time for $\gamma/J = 0.05$, 0.10, 0.15, 0.20, and 0.25. The black dashed lines indicate the logarithmic growth at late times (log-scale time axis). The inserts present the corresponding prefactors. The results are converged for the time step $\delta tJ = 0.5$ and maximum bond dimension $\chi = 50000$.

Ref. [38] or not in the limit $t \to \infty$ is still an open question due to the limited time achieved in our numerical simulation.

5.2 Symmetry-resolved operator entanglement in spin sectors

To understand the logarithmic growth behavior of operator entanglement in the quantum dynamics with SU(2) symmetry, it is useful to consider the symmetry-resolved operator entanglement. We first consider the spin sectors. We show the probabilities p_S of having total spin S in the half system at late times in Fig. 2(a). The half-system total spin is mainly distributed in the low-spin sectors, but as time increases the system has more probabilities in the high-spin sectors. We fit the probability distribution with the trial function

$$p_S = \frac{2S+1}{\sqrt{2\pi\delta^2}}\left[e^{-S^2/2\delta^2} - e^{-(S+1)^2/2\delta^2}\right] \tag{5}$$

with parameter δ and find a good match [see lines in Fig. 2(a)]. Considering the relation $p_S = (2S+1)(p_{S_z=S} - p_{S_z=S+1})$, this suggests that the probability of having magnetization S_z in the half system follows the Gaussian distribution with variance δ in our dissipative quantum many-body dynamics with SU(2) symmetry, like the one observed in the U(1)-symmetric case with dephasing [38].

We also present the symmetry-resolved operator entanglement in different spin sectors in Fig. 2(b). Unlike Ref. [38], where the symmetry-resolved operator entanglement drops to

very small values quickly, here the operator entanglement $S_{\mathrm{op},S}$ remains finite and large at late times, indicating that in addition to the classical Shannon entropy of probability distributions, the symmetry-resolved operator entanglement also have nontrivial contributions to the logarithmic growth of the total operator entanglement in our SU(2)-symmetric case, as we show in Figs. 2(c) and 2(d). The nonvanishing contribution of symmetry-resolved operator entanglement at late times is compatible with the results shown in Refs. [42,43], in which the authors studied the bipartite entanglement of the stationary states for unital quantum channels on a finite chain at $t \to \infty$ and found that the half-system operator entanglement scales logarithmically with the system size for the open quantum many-body systems with SU(2) symmetry. In this $t \to \infty$ limit, the nontrivial Hilbert space structure with dimension $2S+1 > 1$ for spin sectors $S > 0$ leads to the divergent contributions from symmetry-resolved operator entanglement as the system size goes to infinity, otherwise the operator entanglement is fully captured by the classical correlations like the U(1)-symmetric case considered in Ref. [38]. We note that although the operator entanglement shows a logarithmic behavior both in system size in the $t \to \infty$ limit and in time in the limit of infinite system size, it seems that these two phenomena do not have too much connection with each other as the prefactor η in our work is different from those shown in Refs. [42,43].

5.3 Symmetry-resolved operator entanglement in magnetization sectors

Despite the different behavior of symmetry-resolved operator entanglement at late times, the analysis of probabilities p_S suggests that the logarithmic growth behavior of operator entanglement in our dissipative quantum many-body dynamics with SU(2) symmetry can also be understood from the corresponding U(1) subsymmetry by considering the symmetry-resolved operator entanglement in magnetization sectors.

As we expected, the probabilities p_{S_z} indeed are approximately Gaussian at late times, i.e., $p_{S_z} \simeq e^{-S_z^2/2\delta^2}/\sqrt{2\pi\delta^2}$; see Fig. 3(a). In Fig. 3(b), we also present the time dependence of the variance δ, which follows the power law $\sim (tJ)^\alpha$ at late times and explains the logarithmic growth behavior of $-\sum_S p_S \log_2 p_S$ shown in Fig. 2(c). The exponent α in general depends on the dissipation strength and for large γ is close to the value 0.25 predicted for the U(1)-symmetric dissipative quantum dynamics with dephasing [38]; see the insert in Fig. 3(b). Obviously, the classical Shannon entropy of the probabilities in magnetization sectors, $-\sum_{S_z} p_{S_z} \log_2 p_{S_z} \simeq \log_2 \delta + \log_2 \sqrt{2\pi e}$, which follows a logarithmical growth law with prefactor α, also cannot capture the whole prefactor η of the logarithmic growth of operator entanglement at late times; cf. Fig. 1(d).

To identify the behavior of S_{op,S_z}, we first consider the difference of symmetry-resolved operator entanglement between the finite magnetization sector and $S_z = 0$ sector by defining $\Delta S_{\mathrm{op},S_z} \equiv S_{\mathrm{op},S_z} - S_{\mathrm{op},S_z=0}$. The results for $\gamma = 0.05J$ are presented in Fig. 3(c), where as the time increases $\Delta S_{\mathrm{op},S_z}$ decays to very small values. This suggests that the symmetry-resolved operator entanglement S_{op,S_z} will take the same value at long times for all of the magnetization sectors. Moreover, we find that $\Delta S_{\mathrm{op},S_z}$ scaled by $1/S_z^2$ collapses almost onto each other at late times for various magnetization sector S_z and can be captured by the function $(a+btJ)^{-c}$ with $c \approx 1$; see the insert in Fig. 3(c). As the contributions of the symmetry-resolved operator entanglement can be rewritten as $\sum_{S_z} p_{S_z} S_{\mathrm{op},S_z} = S_{\mathrm{op},S_z=0} + \sum_{S_z \neq 0} p_{S_z} \Delta S_{\mathrm{op},S_z}$, where the second term $\sim (tJ)^{2\alpha-c}$ vanishes at long times, this suggests that the late-time behavior of the averaged symmetry-resolved operator entanglement can be captured by $S_{\mathrm{op},S_z=0}$, which, just like the total operator entanglement S_{op}, after the initial rise and fall, increases again in a logarithmic manner at late times; see Fig. 3(d). Together with the classical Shannon entropy of the probability distribution p_{S_z}, this explains the long-time behavior of the total operator entanglement in our SU(2)-symmetric dissipative quantum dynamics.

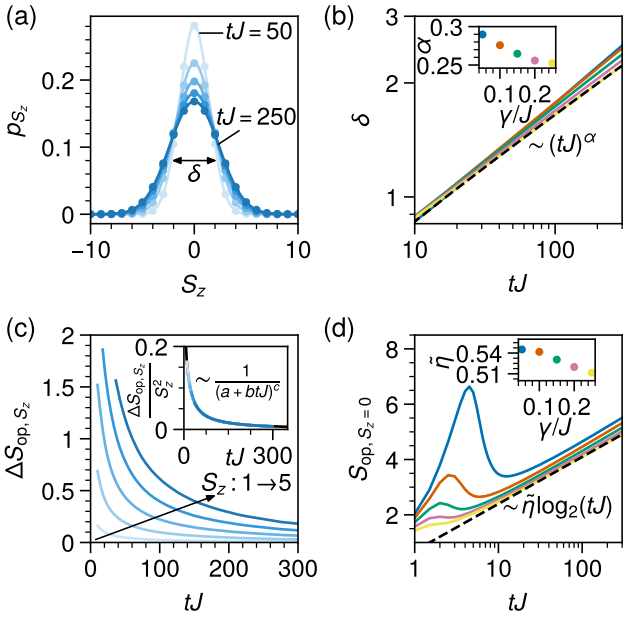

Figure 3: Symmetry-resolved operator entanglement in magnetization sectors. (a) Probabilities p_{S_z} of the infinite chain with magnetization S_z in the half system at increasingly late times ($50 \leq tJ \leq 250$ from light to dark) for $\gamma = 0.05J$. Lines are the Gaussian fits. (b) Variance δ of the Gaussian fits as a function of time for $\gamma/J = 0.05$, 0.10, 0.15, 0.20, and 0.25. The black dashed line indicates $\delta \sim (tJ)^{\alpha}$ at late times (double-log scale). The corresponding exponent α for each γ is shown in the insert. (c) Symmetry-resolved operator entanglement difference $\Delta S_{\mathrm{op},S_z}$ as a function of time for $\gamma = 0.05J$ and $S_z = 1, 2, 3, 4, 5$ (light to dark). The insert shows the data scaled by $1/S_z^2$, and the black line is the fit $(a + btJ)^{-c}$ with $a = 2.4964$, $b = 0.2554$, and $c = 1.1228$. (d) Symmetry-resolved operator entanglement S_{op,S_z} in the magnetization sector $S_z = 0$ as a function of time for various γ. The black dashed line indicates the logarithmic growth of $S_{\mathrm{op},S_z=0}$ at late times (log-scale time axis), with the corresponding prefactors shown in the insert. Here the results are converged for time step $\delta tJ = 0.5$ and maximum bond dimension $\chi = 50000$.

Since the operator entanglement dynamics in our SU(2)-symmetric case can be fully understood from the corresponding U(1) subsymmetry, the above results show evidence that the logarithmic growth of operator entanglement at long times is a generic behavior of the dissipative quantum many-body dynamics with U(1) as the symmetry or subsymmetry. This behavior also holds for more broad dissipations beyond dephasing, which is valid even for the open quantum systems with only U(1) symmetry, as we demonstrated below by breaking the symmetry of our quantum dynamics to U(1).

5.4 Symmetry breaking from SU(2) to U(1)

We consider the quantum dynamics starting from the Néel state $|\psi_0\rangle = \bigotimes_i |\uparrow\rangle_{2i-1} |\downarrow\rangle_{2i}$ and the product state of triplet pairs $|\psi_0\rangle = \bigotimes_i (|\uparrow\rangle_{2i-1} |\downarrow\rangle_{2i} + |\downarrow\rangle_{2i-1} |\uparrow\rangle_{2i})/\sqrt{2}$, which break the SU(2) symmetry to U(1) at the level of initial states. The results for dissipation strength $\gamma = 0.5J$ are presented in Fig. 4. For both initial states, the operator entanglement S_{op} shows the logarithmic growth behavior at late times, although the symmetry-resolved operator entanglement S_{op,S_z} decays to small values at late times for the Néel initial state [see the insert of Fig. 4(a)] while it

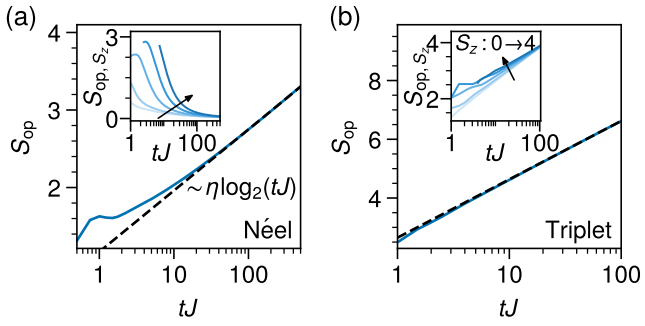

Figure 4: Operator entanglement for quantum dynamics with symmetry being broken to U(1). We consider the Néel initial state in (a) and the product initial state of triplet pairs in (b). The black dashed lines indicate the logarithmic growth of operator entanglement at late times (log-scale time axis), with the prefactor $\eta \approx 0.24$ for (a) and ≈ 0.60 for (b), respectively. The inserts show the time evolution of symmetry-resolved operator entanglement S_{op,S_z} for $S_z = 0, 1, 2, 3, 4$ (from light to dark). Here we set $\gamma = 0.5J$. The time step δtJ is 0.25 for (a) and 0.5 for (b). We choose the maximum bond dimension χ as 4000 for (a) and 12000 for (b).

increases logarithmically for the product initial state of triplet pairs as in the SU(2)-symmetric case [see the insert of Fig. 4(b)]. Since the dissipation in our model (1) is proportional to the dipole interaction between neighbor sites, this demonstrates that the logarithmic growth behavior of operator entanglement at late times holds for more broad dissipations beyond dephasing even for the open quantum many-body dynamics with only U(1) symmetry.

6 Conclusion

In conclusion, we have studied the far-from-equilibrium dynamics of operator entanglement in a dissipative quantum many-body system with SU(2) symmetry. We find that after the initial rise and fall, the operator entanglement increases again in a logarithmic manner at late times. This behavior can be fully understood from the corresponding U(1) subsymmetry by considering the symmetry-resolved operator entanglement, which, unlike the U(1)-symmetric case with dephasing, also contributes to the growth of operator entanglement in addition to the classical Shannon entropy associated with the probabilities for the half system being in different symmetry sectors. Our results show evidence that the logarithmic growth of operator entanglement at late times is a generic behavior of dissipative quantum many-body dynamics with U(1) as the symmetry or subsymmetry and for more broad dissipations beyond dephasing. In the future, it would be interesting to further test this conjecture by investigating more symmetries like SU($N > 2$), SO(N), and SP($2N$). Moreover, in addition to the strong symmetries considered so far, it would be meaningful to study how the presence of weak symmetries impacts the entanglement dynamics of open quantum systems [62, 63].

Acknowledgements

We implement the SU(2) symmetry of tensors using the package `TensorKit.jl` [64]. We acknowledge support from: European Research Council AdG NOQIA; MCIN/AEI (PGC2018-0910.13039/501100011033, CEX2019-000910-S/10.13039/501100011033, Plan National FIDEUA

PID2019-106901GB-I00, Plan National STAMEENA PID2022-139099NB, I00, project funded by MCIN/AEI/10.13039/501100011033 and by the "European Union NextGenerationEU/PRTR" (PRTR-C17.I1), FPI); QUANTERA MAQS PCI2019-111828-2; QUANTERA DYNAMITE PCI2022-132919, QuantERA II Programme co-funded by European Union's Horizon 2020 program under Grant Agreement No 101017733; Ministry for Digital Transformation and of Civil Service of the Spanish Government through the QUANTUM ENIA project call - Quantum Spain project, and by the European Union through the Recovery, Transformation and Resilience Plan - NextGenerationEU within the framework of the Digital Spain 2026 Agenda; Fundació Cellex; Fundació Mir-Puig; Generalitat de Catalunya (European Social Fund FEDER and CERCA program, AGAUR Grant No. 2021 SGR 01452, Quantum CAT\U16-011424, co-funded by ERDF Operational Program of Catalonia 2014-2020); Barcelona Supercomputing Center MareNostrum (FI-2023-3-0024); Funded by the European Union. Views and opinions expressed are however those of the author(s) only and do not necessarily reflect those of the European Union, European Commission, European Climate, Infrastructure and Environment Executive Agency (CINEA), or any other granting authority. Neither the European Union nor any granting authority can be held responsible for them (HORIZON-CL4-2022-QUANTUM-02-SGA PASQuanS2.1, 101113690, EU Horizon 2020 FET-OPEN OPTOlogic, Grant No 899794, QU-ATTO, 101168628), EU Horizon Europe Program (This project has received funding from the European Union's Horizon Europe research and innovation program under grant agreement No 101080086 NeQSTGrant Agreement 101080086 — NeQST); ICFO Internal "QuantumGaudi" project; European Union's Horizon 2020 program under the Marie-Sklodowska-Curie grant agreement No. 847648; "La Caixa" Junior Leaders fellowships, "La Caixa" Foundation (ID 100010434): CF/BQ/PR23/11980043.

A Details on numerical convergence

In this Appendix, we provide more details on the numerical convergence of operator entanglement $S_{\rm op}$ in time step δt and maximum bond dimension χ.

We use the iTEBD algorithm with a Trotter decomposition of the matrix exponential of superoperator $\mathcal{L}_\sharp$ for each time step δt to solve the dissipative quantum many-body dynamics. In order to reach long times, the fourth-order Trotter decomposition [21] is employed:

$$e^{\mathcal{L}_\sharp \delta t} = U(\delta t_1)U(\delta t_2)U(\delta t_3)U(\delta t_2)U(\delta t_1) \tag{6}$$

with

$$U(\delta t_i) = e^{\mathcal{L}_{\sharp,\rm odd}\delta t_i/2} e^{\mathcal{L}_{\sharp,\rm even}\delta t_i} e^{\mathcal{L}_{\sharp,\rm odd}\delta t_i/2} \tag{7}$$

and

$$\delta t_1 = \delta t_2 = \frac{1}{4-4^{1/3}}\delta t, \qquad \delta t_3 = \delta t - 2\delta t_1 - 2\delta t_2. \tag{8}$$

Here $\mathcal{L}_{\sharp,\rm even/odd}$ is the superoperator acting on the even/odd bonds.

As we show in Fig. 5(a), this method allows for the numerical results converged for time steps even up to $\delta t J = 0.5$. In Fig. 5(b), we also present the operator entanglement $S_{\rm op}$ for $\gamma = 0.05J$ with maximum bond dimension $\chi = 50000$ and 60000. The visually indistinguishable lines indicate that the results are already well converged at $\chi = 50000$ up to time $tJ = 300$. For larger $\gamma = 0.10J$, $0.15J$, $0.20J$, and $0.25J$, the operator entanglement will be reduced. Therefore, the maximal bond dimension $\chi = 50000$ is enough to guarantee the numerical convergence for these γ's.

We note that in the plots of prefactor η and offset S_0 of $S_{\rm op}(t\to\infty) = \eta \log_2(tJ) + S_0$ shown in Figs. 1(c) and 1(d), which are obtained by fitting the data set $\{(\log_2(tJ), S_{\rm op}(t))\}$ for $t = t_0, t_0 \pm \delta t$ via a linear function, the results for small $\gamma = 0.05J$ and $\gamma = 0.10J$ exhibit an

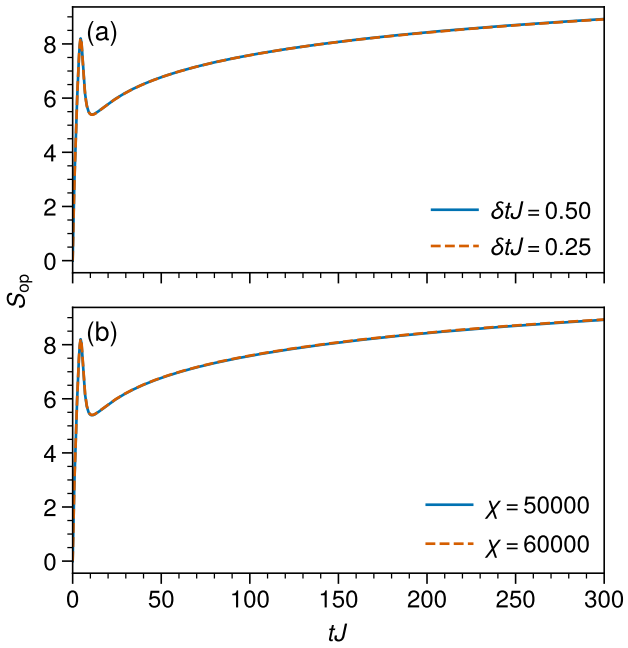

Figure 5: Numerical convergence of operator entanglement S_{op}. (a) Convergence in the time step δt. (b) Convergence in the maximum bond dimension χ. Here we set $\gamma = 0.05J$. The maximum bond dimension χ in (a) is 50000, and the time step δtJ in (b) is 0.5.

artificial wiggle behavior at late times. This arises from numerical errors due to the finite time step and maximal bond dimension. Especially, the later has a more significant influence as the artificial wiggle behavior is highly reduced when the dissipation strength γ increases, which reduces the operator entanglement and increases the accuracy of our numerical simulation with fixed maximal bond dimension $\chi = 50000$. To remove this artificial wiggle behavior of η and S_0 for these small γ's, we could choose a smaller time step and/or a larger maximal bond dimension to further increase the accuracy of our numerical simulations, which, however, requires much more expensive computational resources. Moreover, as we show in the main text, most properties of the operator entanglement, e.g., the late-time logarithmic growth and probability distribution of different symmetry sectors, have already been captured very well in our current numerical simulation. This artificial wiggle behavior at small γ's does not affect our results.

References

[1] I. Bloch, J. Dalibard and S. Nascimbène, *Quantum simulations with ultracold quantum gases*, Nat. Phys. **8**(4), 267 (2012), doi:10.1038/nphys2259.

[2] R. Blatt and C. F. Roos, *Quantum simulations with trapped ions*, Nat. Phys. **8**(4), 277 (2012), doi:10.1038/nphys2252.

[3] B. Gadway and B. Yan, *Strongly interacting ultracold polar molecules*, J. Phys. B: At., Mol. Opt. Phys. **49**(15), 152002 (2016), doi:10.1088/0953-4075/49/15/152002.

[4] A. Browaeys and T. Lahaye, *Many-body physics with individually controlled Rydberg atoms*, Nat. Phys. **16**(2), 132 (2020), doi:10.1038/s41567-019-0733-z.

[5] C. Monroe, W. C. Campbell, L.-M. Duan, Z.-X. Gong, A. V. Gorshkov, P. W. Hess, R. Islam, K. Kim, N. M. Linke, G. Pagano, P. Richerme, C. Senko *et al.*, *Programmable quantum simulations of spin systems with trapped ions*, Rev. Mod. Phys. **93**, 025001 (2021), doi:10.1103/RevModPhys.93.025001.

[6] M. Lewenstein, A. Sanpera, V. Ahufinger, B. Damski, A. Sen(De) and U. Sen, *Ultracold atomic gases in optical lattices: mimicking condensed matter physics and beyond*, Adv. Phys. **56**(2), 243 (2007), doi:10.1080/00018730701223200.

[7] I. Bloch, J. Dalibard and W. Zwerger, *Many-body physics with ultracold gases*, Rev. Mod. Phys. **80**(3), 885 (2008), doi:10.1103/revmodphys.80.885.

[8] O. Dutta, M. Gajda, P. Hauke, M. Lewenstein, D.-S. Lühmann, B. A. Malomed, T. Sowiński and J. Zakrzewski, *Non-standard Hubbard models in optical lattices: a review*, Rep. Prog. Phys. **78**(6), 066001 (2015), doi:10.1088/0034-4885/78/6/066001.

[9] M. Aidelsburger, L. Barbiero, A. Bermudez, T. Chanda, A. Dauphin, D. González-Cuadra, P. R. Grzybowski, S. Hands, F. Jendrzejewski, J. Jünemann, G. Juzeliūnas, V. Kasper *et al.*, *Cold atoms meet lattice gauge theory*, Phil. Trans. R. Soc. A **380**(2216), 20210064 (2021), doi:10.1098/rsta.2021.0064.

[10] A. Polkovnikov, K. Sengupta, A. Silva and M. Vengalattore, *Colloquium: Nonequilibrium dynamics of closed interacting quantum systems*, Rev. Mod. Phys. **83**, 863 (2011), doi:10.1103/RevModPhys.83.863.

[11] A. Eckardt, *Colloquium: Atomic quantum gases in periodically driven optical lattices*, Rev. Mod. Phys. **89**, 011004 (2017), doi:10.1103/RevModPhys.89.011004.

[12] M. Schreiber, S. S. Hodgman, P. Bordia, H. P. Lüschen, M. H. Fischer, R. Vosk, E. Altman, U. Schneider and I. Bloch, *Observation of many-body localization of interacting fermions in a quasirandom optical lattice*, Science **349**(6250), 842 (2015), doi:10.1126/science.aaa7432.

[13] J. Smith, A. Lee, P. Richerme, B. Neyenhuis, P. W. Hess, P. Hauke, M. Heyl, D. A. Huse and C. Monroe, *Many-body localization in a quantum simulator with programmable random disorder*, Nat. Phys. **12**(10), 907 (2016), doi:10.1038/nphys3783.

[14] S. Choi, J. Choi, R. Landig, G. Kucsko, H. Zhou, J. Isoya, F. Jelezko, S. Onoda, H. Sumiya, V. Khemani, C. von Keyserlingk, N. Y. Yao *et al.*, *Observation of discrete time-crystalline order in a disordered dipolar many-body system*, Nature **543**(7644), 221 (2017), doi:10.1038/nature21426.

[15] J. Zhang, P. W. Hess, A. Kyprianidis, P. Becker, A. Lee, J. Smith, G. Pagano, I.-D. Potirniche, A. C. Potter, A. Vishwanath, N. Y. Yao and C. Monroe, *Observation of a discrete time crystal*, Nature **543**(7644), 217 (2017), doi:10.1038/nature21413.

[16] H. Bernien, S. Schwartz, A. Keesling, H. Levine, A. Omran, H. Pichler, S. Choi, A. S. Zibrov, M. Endres, M. Greiner, V. Vuletić and M. D. Lukin, *Probing many-body dynamics on a 51-atom quantum simulator*, Nature **551**(7682), 579 (2017), doi:10.1038/nature24622.

[17] C. J. Turner, A. A. Michailidis, D. A. Abanin, M. Serbyn and Z. Papić, *Weak ergodicity breaking from quantum many-body scars*, Nat. Phys. **14**(7), 745 (2018), doi:10.1038/s41567-018-0137-5.

[18] D. A. Abanin, E. Altman, I. Bloch and M. Serbyn, *Colloquium: Many-body localization, thermalization, and entanglement*, Rev. Mod. Phys. **91**, 021001 (2019), doi:10.1103/RevModPhys.91.021001.

[19] F. Verstraete, V. Murg and J. Cirac, *Matrix product states, projected entangled pair states, and variational renormalization group methods for quantum spin systems*, Adv. Phys. **57**(2), 143 (2008), doi:10.1080/14789940801912366.

[20] U. Schollwöck, *The density-matrix renormalization group in the age of matrix product states*, Ann. Phys. **326**(1), 96 (2011), doi:10.1016/j.aop.2010.09.012.

[21] S. Paeckel, T. Köhler, A. Swoboda, S. R. Manmana, U. Schollwöck and C. Hubig, *Time-evolution methods for matrix-product states*, Ann. Phys. **411**, 167998 (2019), doi:10.1016/j.aop.2019.167998.

[22] G. Vidal, *Efficient Simulation of One-Dimensional Quantum Many-Body Systems*, Phys. Rev. Lett. **93**, 040502 (2004), doi:10.1103/PhysRevLett.93.040502.

[23] D. Perez-Garcia, F. Verstraete, M. M. Wolf and J. I. Cirac, *Matrix product state representations*, Quantum Info. Comput. **7**(5), 401 (2007), doi:10.5555/2011832.2011833.

[24] N. Schuch, M. M. Wolf, F. Verstraete and J. I. Cirac, *Entropy Scaling and Simulability by Matrix Product States*, Phys. Rev. Lett. **100**, 030504 (2008), doi:10.1103/PhysRevLett.100.030504.

[25] P. Calabrese and J. Cardy, *Evolution of entanglement entropy in one-dimensional systems*, J. Stat. Mech.: Theory Exp. **2005**(04), P04010 (2005), doi:10.1088/1742-5468/2005/04/p04010.

[26] M. Fagotti and P. Calabrese, *Evolution of entanglement entropy following a quantum quench: Analytic results for the xy chain in a transverse magnetic field*, Phys. Rev. A **78**, 010306 (2008), doi:10.1103/PhysRevA.78.010306.

[27] V. Alba and P. Calabrese, *Entanglement and thermodynamics after a quantum quench in integrable systems*, Proc. Natl. Acad. Sci. U.S.A. **114**(30), 7947 (2017), doi:10.1073/pnas.1703516114.

[28] A. Lukin, M. Rispoli, R. Schittko, M. E. Tai, A. M. Kaufman, S. Choi, V. Khemani, J. Léonard and M. Greiner, *Probing entanglement in a many-body-localized system*, Science **364**(6437), 256 (2019), doi:10.1126/science.aau0818.

[29] M. Zwolak and G. Vidal, *Mixed-State Dynamics in One-Dimensional Quantum Lattice Systems: A Time-Dependent Superoperator Renormalization Algorithm*, Phys. Rev. Lett. **93**, 207205 (2004), doi:10.1103/PhysRevLett.93.207205.

[30] F. Verstraete, J. J. García-Ripoll and J. I. Cirac, *Matrix Product Density Operators: Simulation of Finite-Temperature and Dissipative Systems*, Phys. Rev. Lett. **93**(20), 207204 (2004), doi:10.1103/physrevlett.93.207204.

[31] A. H. Werner, D. Jaschke, P. Silvi, M. Kliesch, T. Calarco, J. Eisert and S. Montangero, *Positive Tensor Network Approach for Simulating Open Quantum Many-Body Systems*, Phys. Rev. Lett. **116**(23), 237201 (2016), doi:10.1103/physrevlett.116.237201.

[32] P. Zanardi, C. Zalka and L. Faoro, *Entangling power of quantum evolutions*, Phys. Rev. A **62**, 030301 (2000), doi:10.1103/PhysRevA.62.030301.

[33] P. Zanardi, *Entanglement of quantum evolutions*, Phys. Rev. A **63**, 040304 (2001), doi:10.1103/PhysRevA.63.040304.

[34] X. Wang and P. Zanardi, *Quantum entanglement of unitary operators on bipartite systems*, Phys. Rev. A **66**, 044303 (2002), doi:10.1103/PhysRevA.66.044303.

[35] T. Prosen and I. Pižorn, *Operator space entanglement entropy in a transverse Ising chain*, Phys. Rev. A **76**, 032316 (2007), doi:10.1103/PhysRevA.76.032316.

[36] I. Pižorn and T. Prosen, *Operator space entanglement entropy in XY spin chains*, Phys. Rev. B **79**, 184416 (2009), doi:10.1103/PhysRevB.79.184416.

[37] J. Dubail, *Entanglement scaling of operators: a conformal field theory approach, with a glimpse of simulability of long-time dynamics in 1 + 1d*, J. Phys. A: Math. Theor. **50**(23), 234001 (2017), doi:10.1088/1751-8121/aa6f38.

[38] D. Wellnitz, G. Preisser, V. Alba, J. Dubail and J. Schachenmayer, *Rise and Fall, and Slow Rise Again, of Operator Entanglement under Dephasing*, Phys. Rev. Lett. **129**, 170401 (2022), doi:10.1103/PhysRevLett.129.170401.

[39] S. Choi, C. J. Turner, H. Pichler, W. W. Ho, A. A. Michailidis, Z. Papić, M. Serbyn, M. D. Lukin and D. A. Abanin, *Emergent SU(2) Dynamics and Perfect Quantum Many-Body Scars*, Phys. Rev. Lett. **122**(22), 220603 (2019), doi:10.1103/PhysRevLett.122.220603.

[40] E. Ilievski, J. De Nardis, S. Gopalakrishnan, R. Vasseur and B. Ware, *Superuniversality of Superdiffusion*, Phys. Rev. X **11**, 031023 (2021), doi:10.1103/PhysRevX.11.031023.

[41] S. Majidy, A. Lasek, D. A. Huse and N. Yunger Halpern, *Non-abelian symmetry can increase entanglement entropy*, Phys. Rev. B **107**, 045102 (2023), doi:10.1103/PhysRevB.107.045102.

[42] Y. Li, F. Pollmann, N. Read and P. Sala, *Highly entangled stationary states from strong symmetries*, Phys. Rev. X **15**, 011068 (2025), doi:10.1103/PhysRevX.15.011068.

[43] A. Moharramipour, L. A. Lessa, C. Wang, T. H. Hsieh and S. Sahu, *Symmetry-enforced entanglement in maximally mixed states*, PRX Quantum **5**, 040336 (2024), doi:10.1103/PRXQuantum.5.040336.

[44] N. Laflorencie and S. Rachel, *Spin-resolved entanglement spectroscopy of critical spin chains and Luttinger liquids*, J. Stat. Mech: Theory Exp. **2014**(11), P11013 (2014), doi:10.1088/1742-5468/2014/11/P11013.

[45] M. Goldstein and E. Sela, *Symmetry-Resolved Entanglement in Many-Body Systems*, Phys. Rev. Lett. **120**, 200602 (2018), doi:10.1103/PhysRevLett.120.200602.

[46] J. C. Xavier, F. C. Alcaraz and G. Sierra, *Equipartition of the entanglement entropy*, Phys. Rev. B **98**, 041106 (2018), doi:10.1103/PhysRevB.98.041106.

[47] J. De Nardis, S. Gopalakrishnan, R. Vasseur and B. Ware, *Stability of superdiffusion in nearly integrable spin chains*, Phys. Rev. Lett. **127**, 057201 (2021), doi:10.1103/PhysRevLett.127.057201.

[48] P. W. Claeys, A. Lamacraft and J. Herzog-Arbeitman, *Absence of Superdiffusion in Certain Random Spin Models*, Phys. Rev. Lett. **128**, 246603 (2022), doi:10.1103/PhysRevLett.128.246603.

[49] G. Vidal, *Classical Simulation of Infinite-Size Quantum Lattice Systems in One Spatial Dimension*, Phys. Rev. Lett. **98**, 070201 (2007), doi:10.1103/PhysRevLett.98.070201.

[50] R. Orús and G. Vidal, *Infinite time-evolving block decimation algorithm beyond unitary evolution*, Phys. Rev. B **78**, 155117 (2008), doi:10.1103/PhysRevB.78.155117.

[51] G. Vidal and R. F. Werner, *Computable measure of entanglement*, Phys. Rev. A **65**, 032314 (2002), doi:10.1103/PhysRevA.65.032314.

[52] M. B. Plenio, *Logarithmic Negativity: A Full Entanglement Monotone That is not Convex*, Phys. Rev. Lett. **95**, 090503 (2005), doi:10.1103/PhysRevLett.95.090503.

[53] T. Zhou and D. J. Luitz, *Operator entanglement entropy of the time evolution operator in chaotic systems*, Phys. Rev. B **95**, 094206 (2017), doi:10.1103/PhysRevB.95.094206.

[54] V. Alba, J. Dubail and M. Medenjak, *Operator Entanglement in Interacting Integrable Quantum Systems: The Case of the Rule 54 Chain*, Phys. Rev. Lett. **122**, 250603 (2019), doi:10.1103/PhysRevLett.122.250603.

[55] G. Styliaris, N. Anand and P. Zanardi, *Information Scrambling over Bipartitions: Equilibration, Entropy Production, and Typicality*, Phys. Rev. Lett. **126**, 030601 (2021), doi:10.1103/PhysRevLett.126.030601.

[56] H. Barghathi, C. M. Herdman and A. Del Maestro, *Rényi Generalization of the Accessible Entanglement Entropy*, Phys. Rev. Lett. **121**, 150501 (2018), doi:10.1103/PhysRevLett.121.150501.

[57] H. Barghathi, E. Casiano-Diaz and A. Del Maestro, *Operationally accessible entanglement of one-dimensional spinless fermions*, Phys. Rev. A **100**, 022324 (2019), doi:10.1103/PhysRevA.100.022324.

[58] G. Parez, R. Bonsignori and P. Calabrese, *Quasiparticle dynamics of symmetry-resolved entanglement after a quench: Examples of conformal field theories and free fermions*, Phys. Rev. B **103**, L041104 (2021), doi:10.1103/PhysRevB.103.L041104.

[59] A. Rath, V. Vitale, S. Murciano, M. Votto, J. Dubail, R. Kueng, C. Branciard, P. Calabrese and B. Vermersch, *Entanglement barrier and its symmetry resolution: Theory and experimental observation*, PRX Quantum **4**, 010318 (2023), doi:10.1103/PRXQuantum.4.010318.

[60] Y. Li, P. Sala and F. Pollmann, *Hilbert space fragmentation in open quantum systems*, Phys. Rev. Res. **5**, 043239 (2023), doi:10.1103/PhysRevResearch.5.043239.

[61] S. Murciano, J. Dubail and P. Calabrese, *More on symmetry resolved operator entanglement*, J. Phys. Math. Theor. **57**(14), 145002 (2024), doi:10.1088/1751-8121/ad30d1.

[62] B. Buča and T. Prosen, *A note on symmetry reductions of the Lindblad equation: transport in constrained open spin chains*, New J. Phys. **14**(7), 073007 (2012), doi:10.1088/1367-2630/14/7/073007.

[63] K. Kawabata, A. Kulkarni, J. Li, T. Numasawa and S. Ryu, *Symmetry of Open Quantum Systems: Classification of Dissipative Quantum Chaos*, PRX Quantum **4**, 030328 (2023), doi:10.1103/PRXQuantum.4.030328.

[64] J. Haegeman, *TensorKit.jl: A Julia package for large-scale tensor computations, with a hint of category theory*, https://github.com/Jutho/TensorKit.jl.